Supplementary Material (ESI) for Chemical Communications

Supporting Information for:

A Natural Abundance ^{33}S Solid-State NMR Study of Layered Transition Metal Disulfides at Ultrahigh Magnetic Field

by Andre Sutrisno,[†] Victor V. Terskikh[‡] and Yining Huang[†,*]

Contribution from:

[†] *Department of Chemistry, The University of Western Ontario, London, Ontario, Canada N6A 5B7, and* [‡]*Steacie Institute for Molecular Sciences, National Research Council, Ottawa, Ontario, Canada K1A 0R6.*

Table S1. Experimental and calculated ^{33}S NMR parameters.

Compound	Method	C_Q (MHz)[a]	η_Q[b]
2H-MoS_2	experimental	9.3 (8)	0
	calculated[c]	7.53	0
2H-WS_2	experimental	7.9 (5)	0
	calculated	6.66	0
1T-ZrS_2	experimental	0.5 (5)	0
	calculated	0.54	0
1T-TiS_2	experimental	1.8 (5)	0
	calculated	1.08	0
1T-TaS_2	experimental	4.5 (5)	0.50 (10)
	calculated	3.85	0

[a] $C_Q = eQV_{ZZ}/h$; [b] $\eta_Q = (V_{XX} - V_{YY})/V_{ZZ}$ where $|V_{ZZ}| \geq |V_{YY}| \geq |V_{XX}|$. η_Q was set to 0 for all the metal disulfides due to the C_3 site symmetry; [c] see experimental section for more details of the calculations.

Table S2. Detailed experimental conditions for ^{33}S NMR.

Sample	Type of experiment	B_0 (T)	90° pulse length (µs)	SW (kHz)	recycle delay (s)	τ_a (µs)	M (# of loops)	τ_1 (µs)	τ_2 (µs)	τ_3 (µs)	τ_4 (µs)	# scans
2H-MoS_2	static QCPMG	21.1	5	500	5	200	64	29	30	30	30	7 x 3600
2H-WS_2	static QCPMG	21.1	10	500	5	250	128	29	30	30	30	8 x 3600
1T-ZrS_2	static Hahn-echo	21.1	5	100	5	-	-	100	-	-	-	9850
	1 pulse MAS at 6 kHz	21.1	4	100	10[a]	-	-	-	-	-	-	313
1T-TiS_2	static QCPMG	9.4	3	100	3	1000	19	25	26	26	27	48912
	static QCPMG	21.1	5	200	3	1000	64	29	30	30	30	1024
	static Hahn-echo	21.1	5	200	10[a]	-	-	50	-	-	-	4773
	Hahn-echo MAS at 6 kHz	21.1	5	200	3	-	-	-	-	-	-	20400
1T-TaS_2	static QCPMG	21.1	5	250	1	250	128	29	30	30	30	8 x 4096
	static Hahn-echo	21.1	5	250	1	-	-	55	-	-	-	58827

[a] The recycle delay of 3 seconds was sufficient for almost complete relaxation.

Experimental Section:

Materials. The samples of MoS_2, WS_2, ZrS_2, TiS_2 and TaS_2 were purchased from STREM Chemicals, Inc. and used as received. The identity, purity and crystallinity of the samples were confirmed by powder X-ray diffraction (see Figure S6).

Powder X-ray diffraction. Powder X-ray diffraction patterns were recorded on a Rigaku diffractometer equipped with a graphite monochromator using Co Kα radiation (λ = 1.7902 Å). The step size used was 0.02° and scan range was from 5 - 65° (2θ) with a rate of 10°/minute.

Solid-state NMR spectroscopy.

a. Experiments at 21.1 T. Solid-state ^{33}S NMR experiments were performed on a 900 MHz Bruker Avance II spectrometer at the *National Ultrahigh-field NMR Facility for Solids* in Ottawa, Canada, operating at a frequency of 69.05 MHz. A 7.0 mm single channel Bruker MAS probe was used for both static and MAS experiments. The samples were ground into a fine powder and then packed into 7.0 mm o.d. Bruker zirconia rotors. For MoS_2 and WS_2, the samples were first pressed into pallets under hydraulic pressure and then packed in the rotor to fit in more than double amount of the sample. Experimental setup, pulse calibration and referencing were done using either 1M Cs_2SO_4 solution (δ_{iso} = 333 ppm) or solid CaS (δ_{iso} = -28.5 ppm), both can act as a secondary standard to neat CS_2 at 0.0 ppm. ^{33}S static NMR spectra were collected using the conventional quadrupolar Carr-Purcell-Meiboom-Gill (QCPMG) pulse sequence, while a single pulse or a rotor-synchronized Hahn-echo pulse experiment was carried out to acquire MAS spectra. The Hahn-echo pulse sequence has the form (π/2) - τ - (π) - τ - acq, where τ represents inter-pulse delays of 20 - 50 μs. For QCPMG, the frequency-stepped

technique was used when the breadth of the CT spectra exceeded the pulse width excitation profile. The sub-spectra with different frequency offsets were co-added in frequency scale (Hertz). The resulting spectrum was then treated and referenced as a single spectrum. The spectrometer conditions used are summarized in Table S2. Since the samples have no protons, proton-decoupling was not applied.

b. Experiments at 9.4 T. ^{33}S SSNMR experiments were also carried out on a Varian InfinityPlus spectrometer with an Oxford 9.4 T wide-bore magnet, operating at resonance frequency of 30.65 MHz. A Varian/Chemagnetics 7.5 mm HXY MAS probe was used. The samples were ground into fine powders and packed into 7.5 mm o.d. zirconia rotors. Experimental setup, pulse calibration and referencing were done using either 1M Cs_2SO_4 solution (δ_{iso} = 333 ppm) or solid CaS (δ_{iso} = -28.5 ppm), both acting as secondary standard to neat CS_2 at 0.0 ppm. ^{33}S static NMR spectra were collected using the QCPMG pulse sequence (see Table S2 for details).

NMR spectral simulations. All NMR parameters including C_Q, η_Q, δ_{iso}, Ω, and κ were determined by analytical simulations of NMR spectra using the WSOLIDS1[1] simulation package. The experimental error for each measured parameter was determined by visual comparison of experimental spectra with simulations. The parameter of concern was varied bidirectionally starting from the best fit value and all other parameters were kept constant, until noticeable differences between the spectra were observed.

Theoretical calculations. First-principles (*ab initio*) calculations based on plane wave-pseudo potential Density Functional Theory were conducted using CASTEP (version 4.3)[2, 3] program setup by the Materials Studio graphical user interface, running on a single CPU. The NMR module[4-6] was used to calculate the ^{33}S EFG and CSA tensors.

The gauge-including projector augmented-wave (GIPAW) method which uses pseudo potentials and plane wave basis sets to describe three dimensional lattices in crystalline materials was utilized. Unit cell parameters and atomic coordinates were taken from corresponding crystal structures.[7-11] The Generalized Gradient Approximation (GGA) with Perdew, Burke and Ernzerhof (PBE) functional was used for all the calculations.[12, 13] The principal components of the EFG tensor (V_{XX}, V_{YY}, V_{ZZ}) were converted to quadrupole coupling constant C_Q and asymmetry parameter η_Q according to the following definition: $|V_{ZZ}| \geq |V_{YY}| \geq |V_{XX}|$; C_Q (in Hz) = $(eV_{ZZ}Q/h)$ x 9.71736 x 10^{21} V·m^{-2}; $\eta_Q = (V_{XX} - V_{YY})/V_{ZZ}$, where e is the electric charge; Q is the nuclear quadrupole moment [$Q(^{33}S)$ = -0.0678 barn][14].

References:

1. Eichele, K.; Wasylishen, R. E. *WSolids1: Solid-State NMR Spectrum Simulation*, v. 1.17.30; 2001.
2. Clark, S. J.; Segall, M. D.; Pickard, C. J.; Hasnip, P. J.; Probert, M. I. J.; Refson, K.; Payne, M. C., *Z. Kristallogr.* **2005,** 220, (5-6), 567-570.
3. Segall, M. D.; Lindan, P. J. D.; Probert, M. J.; Pickard, C. J.; Hasnip, P. J.; Clark, S. J.; Payne, M. C., *J. Phys.: Condens. Matter* **2002,** 14, (11), 2717-2744.
4. Pickard, C. J.; Mauri, F., *Phys. Rev. B: Condens. Matter Mater. Phys.* **2001,** 63, (24), 245101/1-245101/13.
5. Profeta, M.; Mauri, F.; Pickard, C. J., *J. Am. Chem. Soc.* **2003,** 125, (2), 541-548.
6. Yates, J. R.; Pickard, C. J.; Mauri, F., *Phys. Rev. B: Condens. Matter Mater. Phys.* **2007,** 76, (2), 024401/1-024401/11.
7. Jellinek, F., *Arkiv. Kemi* **1963,** 20, 447-80.
8. Bronsema, K. D.; De Boer, J. L.; Jellinek, F., *Z. Anorg. Allg. Chem.* **1986,** 540-541, 15-17.
9. Schutte, W. J.; De Boer, J. L.; Jellinek, F., *J. Solid State Chem.* **1987,** 70, (2), 207.
10. Kusawake, T.; Takahashi, Y.; Wey, M. Y.; Ohshima, K.-I., *J. Phys.: Condens. Matter* **2001,** 13, (44), 9913-9921.
11. Spijkerman, A.; de Boer, J. L.; Meetsma, A.; Wiegers, G. A.; van Smaalen, S., *Phys. Rev. B: Condens. Matter* **1997,** 56, (21), 13757-13767.
12. Perdew, J. P.; Burke, K.; Ernzerhof, M., *Phys. Rev. Lett.* **1997,** 78, (7), 1396.
13. Perdew, J. P.; Burke, K.; Ernzerhof, M., *Phys. Rev. Lett.* **1996,** 77, (18), 3865-3868.
14. Pyykko, P., *Mol. Phys.* **2001,** 99, (19), 1617-1629.

Figure S1. Structure of (a) 2H-MoS_2 / WS_2 and (b) 1T-ZrS_2 / TiS_2 / TaS_2

Different views of MS_2: *1)* view down c axis, *2)* metal coordination site, *3)* unit cell, *4)* view down b axis, *5)* packing of layered MS_2.

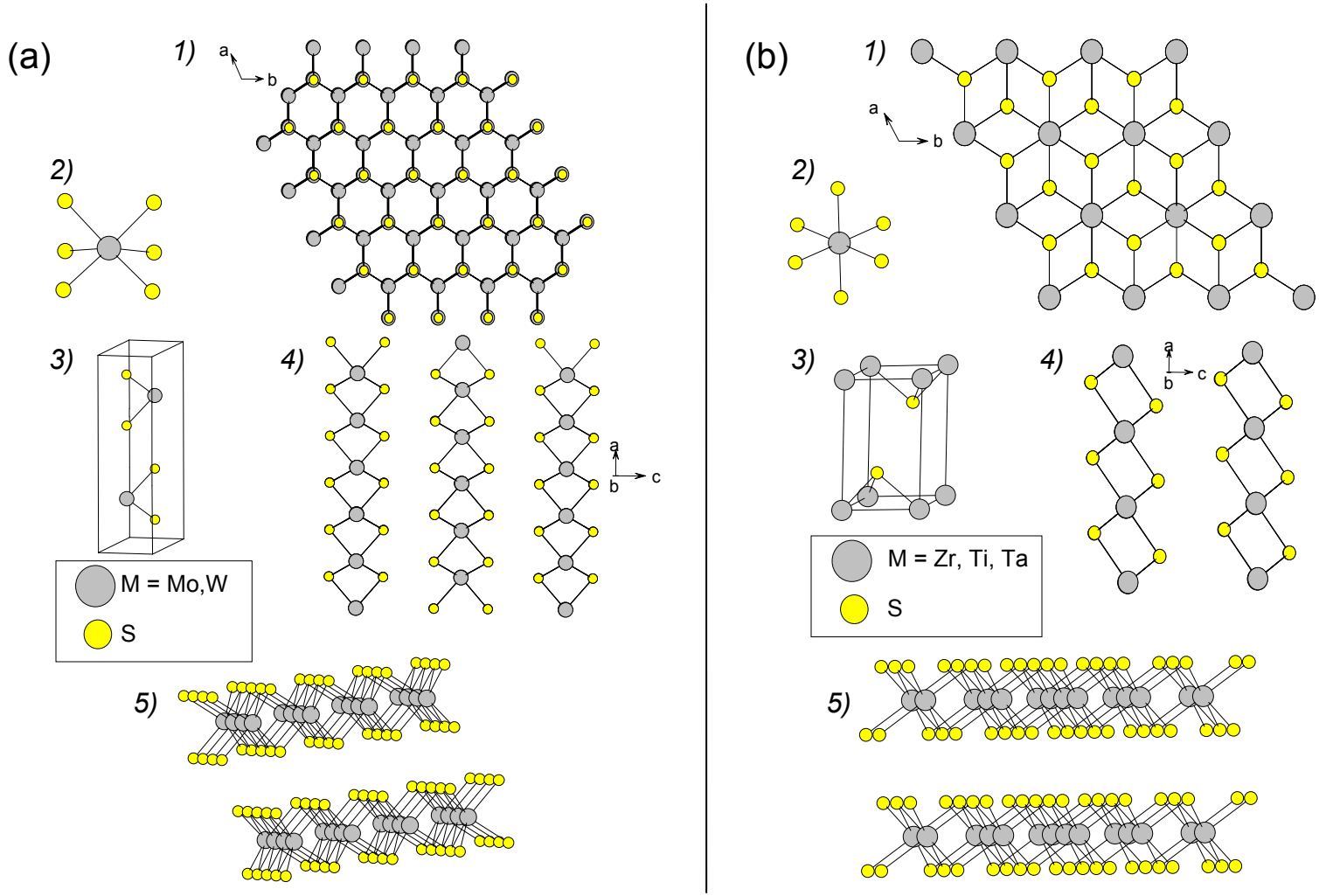

Figure S2. ^{33}S static frequency-stepped acquisition QCPMG spectra of 2H-MoS_2 at 21.1 T.

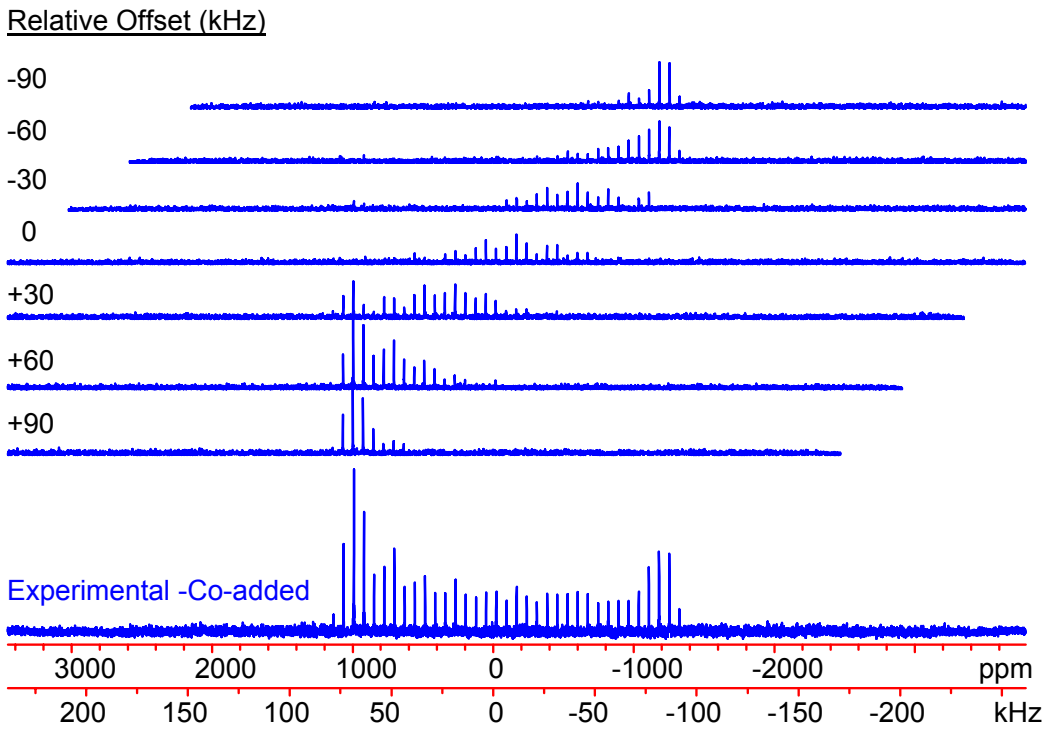

7 pieces for qcpmg (5 hours each)

Figure S3. ^{33}S static frequency-stepped acquisition QCPMG spectra of 2H-WS_2 at 21.1 T.

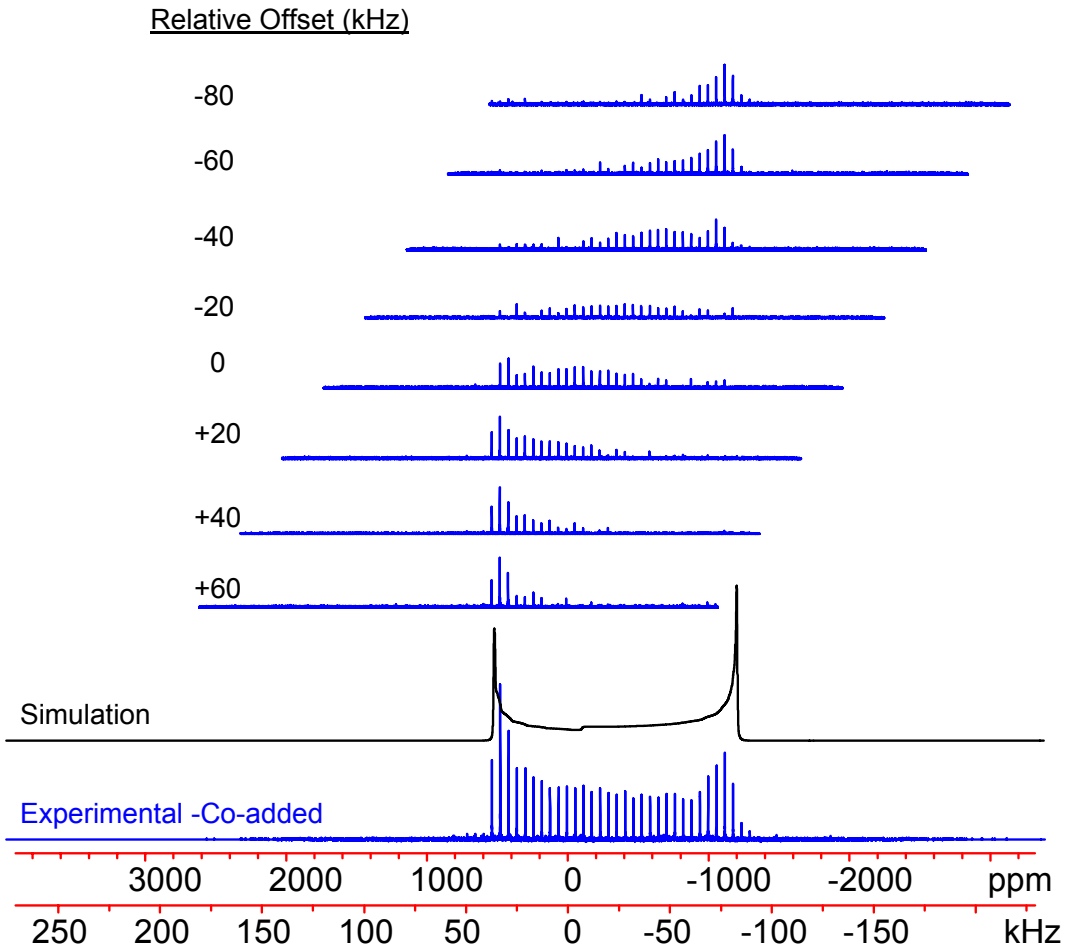

8 pieces for qcpmg (3 hours each)

Figure S4. a) ^{33}S NMR spectra of 1T-TiS_2 at 21.1 T. b) ^{33}S static QCPMG spectra of 1T-TiS_2 at 9.4 T.

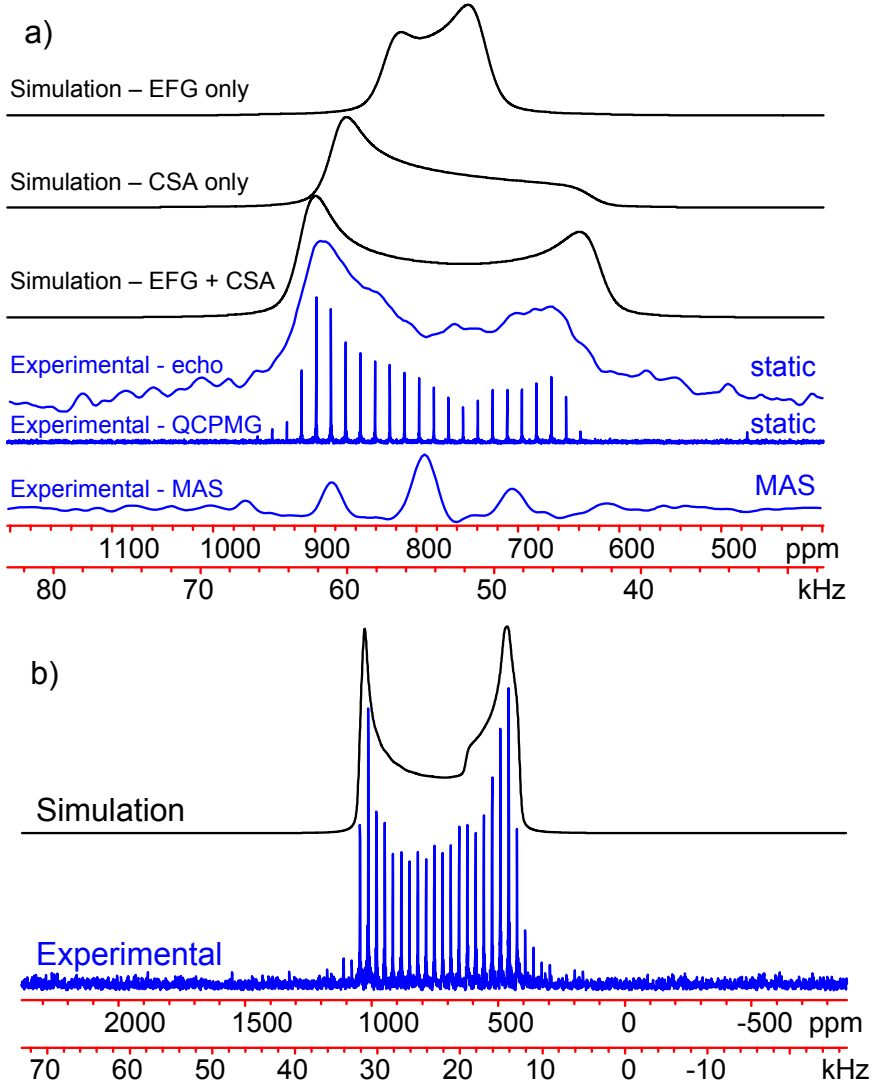

Figure S5. ^{33}S static NMR spectra of 1T-TaS_2 at 21.1 T.

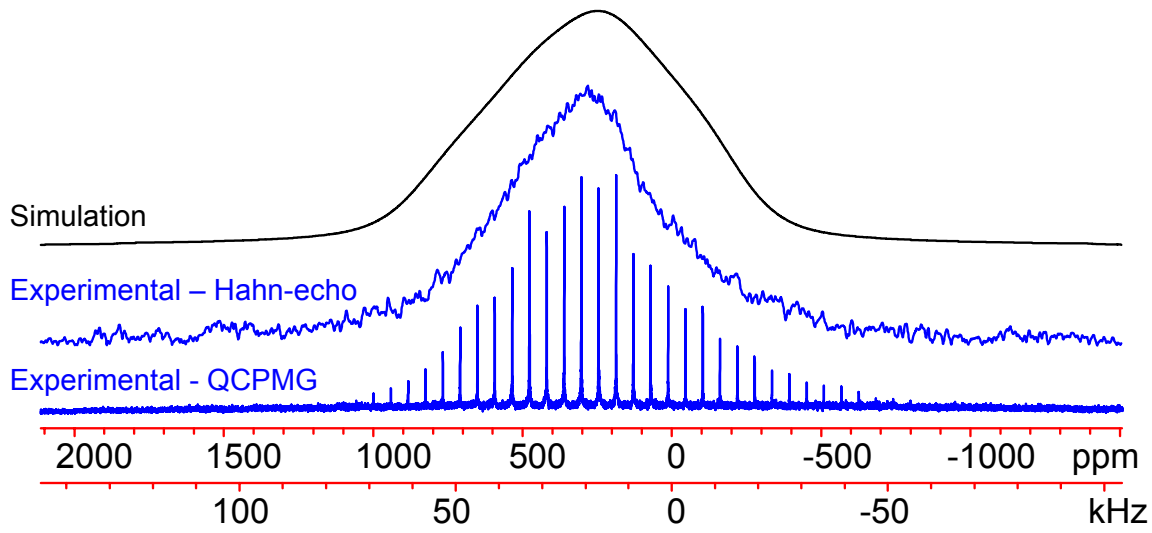

Figure S6. Powder XRD patterns of MS_2

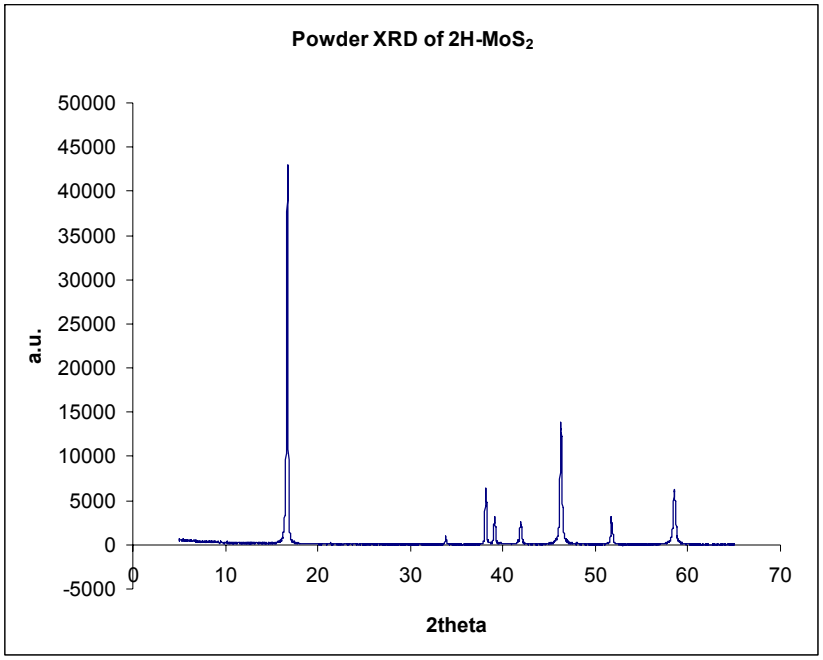

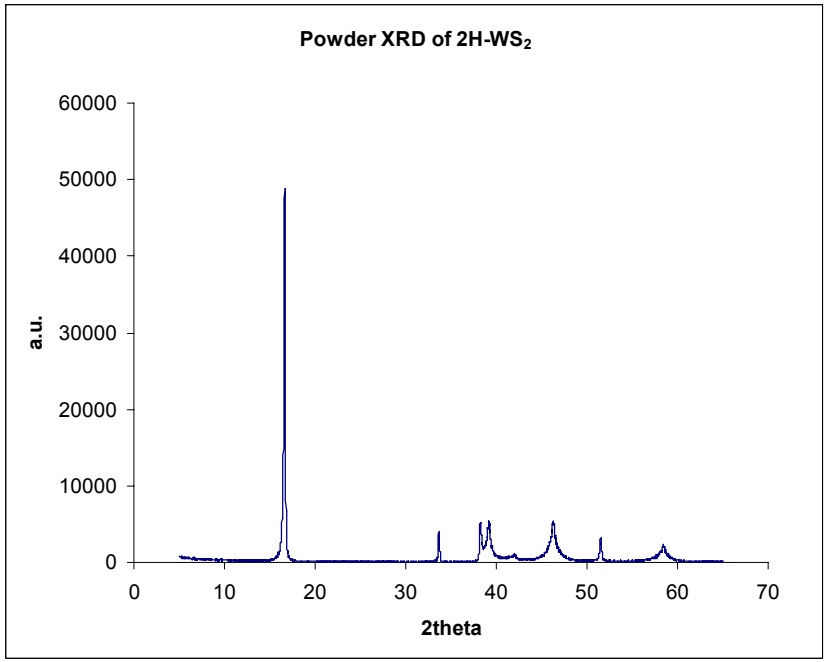

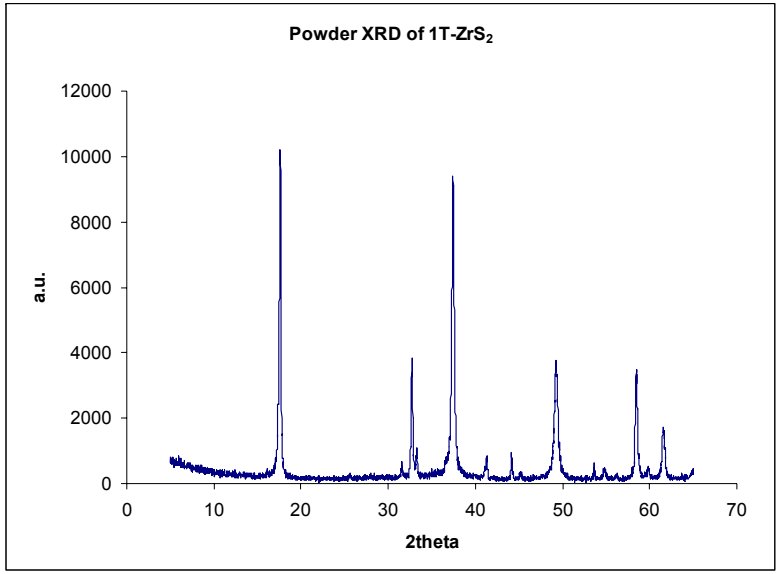
Powder XRD of 1T-ZrS2
a.u.
2theta
12000
10000
8000
6000
4000
2000
0
0
10
20
30
40
50
60
70

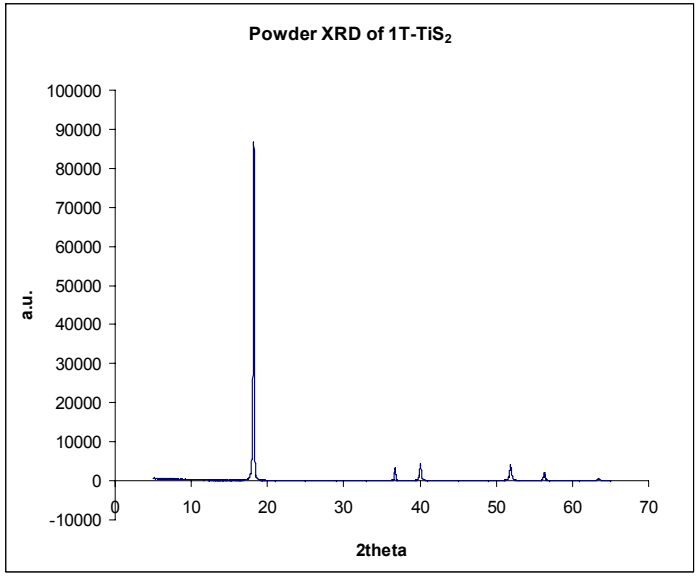
Powder XRD of 1T-TiS2
a.u.
2theta
100000
90000
80000
70000
60000
50000
40000
30000
20000
10000
0
-10000
0
10
20
30
40
50
60
70

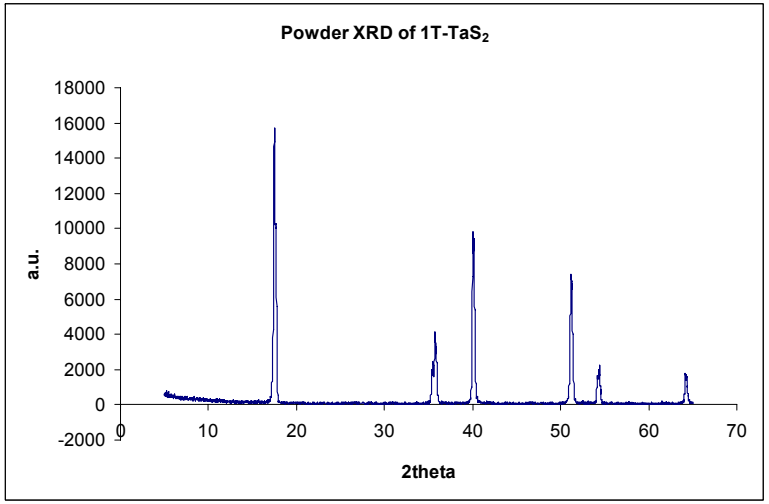
Powder XRD of 1T-TaS2
a.u.
2theta
18000
16000
14000
12000
10000
8000
6000
4000
2000
0
-2000
0
10
20
30
40
50
60
70